Origin of ferroelectric polarization in spiral magnetic structure of $MnWO_4$

K. V. Shanavas,[1] Debraj Choudhury,[2,3] I. Dasgupta,[4,5] Surinder M. Sharma,[1] and D. D. Sarma[2]
[1]*High Pressure Physics Division, Bhabha Atomic Research Centre, Mumbai 400 085, India*
[2]*Solid State and Structural Chemistry Unit, Indian Institute of Science, Bangalore 560012, India*
[3]*Department of Physics, Indian Institute of Science, Bangalore 560012, India*
[4]*Department of Physics, Indian Institute of Technology Bombay, Powai, Mumbai 400 076, India*
[5]*Department of Solid State Physics and Centre for Advanced Materials, Indian Association for the Cultivation of Science, Jadavpur, Kolkata 700 032, India*
(Received 30 April 2010; published 14 June 2010)

Magnetism and the origin of ferroelectricity in the multiferroic $MnWO_4$ are studied using *ab initio* electronic-structure calculations, correctly reproducing the magnetic ground state. The calculated ferroelectric polarization is in good agreement with experiments. Our results reveal that spin-orbit interaction is necessary and sufficient to explain the observed ferroelectric polarization, establishing an entirely electronic origin of ferroelectricity in $MnWO_4$. The origin of spin-orbit interaction in this compound with a nominally d^5 $L=0$ orbitally quenched state is elucidated by analyzing results of x-ray absorption spectroscopy.

DOI: 10.1103/PhysRevB.81.212406 PACS number(s): 75.80.+q, 71.20.−b, 77.80.−e, 78.70.Dm

Multiferroics are materials where magnetism coexists with ferroelectricity.[1–3] *Improper ferroelectrics* form an important subset where ferroelectricity is induced by an inversion symmetry breaking magnetic ordering. In collinear spin systems this can happen via symmetric exchange striction effects as observed in YMn_2O_5,[4] Ca_3CoMnO_6,[5] etc. Spin systems with cycloidal spiral magnetic structures can also develop finite polarization (P) if the spin rotation axis $\hat{e}$ does not coincide with the propagation vector $\mathbf{Q}$, with $P \propto \hat{e} \times \mathbf{Q}$,[6] e.g., in $TbMnO_3$, $Ni_3V_2O_8$, $CoCr_2O_4$, and $MnWO_4$.[1,7–9] In these spiral magnets, the relevant exchange striction is associated with the antisymmetric part of the exchange coupling,[10] known as the Dzyaloshinskii-Moriya interaction (DMI). As a result, spin-orbit interaction is indispensable in generating electric dipole moments.

Model Hamiltonian studies of spin-spiral multiferroic compounds have provided two different pictures. The first is based on purely electronic mechanisms,[6,11] promoted by the spin-orbit interaction (SOI) that modifies the hybridization of the electronic orbitals in such a way as to shift the center of charge even if the ions are not displaced from their centrosymmetric positions. The second one relies on *lattice mechanism* where DMI not only induces ferroelectric lattice displacements but also helps to stabilize helical magnetic structures.[12] Recent *ab initio* calculations have provided evidence for both the mechanisms[13–15] in spin spiral systems.

Among cycloidal spiral magnets, the origin of ferroelectric polarization in the compound $MnWO_4$ (Refs. 9 and 16–18) is particularly intriguing since the role of SOI is not clear. The system is believed to be in $Mn^{2+}(3d^5)O^{2-}(2p^6)$ configuration which would be expected to have quenched orbital moment, similar to the recently discovered spin spiral multiferroic $FeVO_4$.[19] Model Hamiltonian calculations suggest that either mixing of ligand p orbitals with d orbitals or t_{2g}-e_g orbital mixing by SOI can lead to electric polarization in systems with nonzero spin with an arbitrary d^n configuration.[11] Therefore, first-principles electronic-structure calculations are important to assess the role of SOI in $MnWO_4$. In addition, x-ray absorption spectroscopy is known to be a powerful probe to understand details of electronic interactions, including multipole Coulomb interaction, SOI, and hopping between transition metal d and O p states. Therefore, we have probed the Mn $3d$ states using Mn $2p$-$3d$ absorption edge spectrum. In this Brief Report, we present results of first-principles electronic-structure calculations and x-ray absorption (XA) spectroscopy to understand the electronic structure and the origin of ferroelectric polarization in the multiferroic $MnWO_4$.

$MnWO_4$ crystallizes in the wolframite structure,[20] with a monoclinic space group $P2/c$, shown in Fig. 1(a). Each unit cell includes two Mn^{2+} ions that are interconnected via the common edges of distorted MnO_6 octahedra forming zigzag chains along the c axis. The W^{6+} ions that alternately stack along the a axis are also coordinated by distorted O octahedra, corner sharing with the MnO_6 octahedra. This compound exhibits three successive magnetic phase transitions at 7.6 K(T_{N1}), 12.7 K(T_{N2}) and 13.5 K(T_{N3}).[20,21] Incommensurate collinear sinusoidal magnetic structure is stable in the antiferromagnetic (AF3) phase ($T_{N2} < T < T_{N3}$) with the propagation vector $\mathbf{q}$ approximately equal to $(-0.214, 1/2, 0.457)$. The magnetic moments of Mn^{2+} align along the easy axis that lie in the ac plane forming an angle

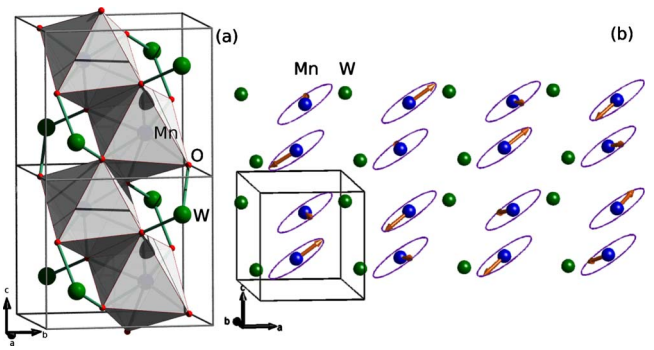

FIG. 1. (Color online) (a) Crystal structure of $MnWO_4$ and (b) elliptical spiral spin structure in AF2 phase of $MnWO_4$. The arrows represent the spins and the ellipses indicate their plane of rotation

$\alpha \simeq 35°$ with the a axis. Below T_{N2}, an incommensurate elliptical spiral magnetic structure (AF2 phase) appears coplanar in the plane spanned by the easy direction (defined by $\alpha=35°$ in the ac plane) and [010] [see Fig. 1(b)]. It has a finite component of moment along the b axis, in general, and with $\mathbf{q}$ almost identical to that in AF3. The magnetic structure below T_{N1} again becomes collinear (AF1) but with a commensurate wave vector $\mathbf{q}=(\pm 1/4, 1/2, 1/2)$. The spontaneous electric polarization along b axis occurs only in the spiral AF2 phase, suggesting that noncollinear spin configuration plays a key role in the occurrence of electric polarization.

First-principles density-functional-theory calculations are performed using the Vienna *ab initio* simulation package (VASP),[22] within the projector augmented wave method. We use local density approximation (LDA) with on-site coulomb interactions, $U=4$ eV applied to the d states of Mn using an approach described by Dudarev *et al.*[23] We approximate the incommensurate wave vector $\mathbf{q} \simeq (-0.214, 1/2, 0.457)$ by a commensurate one, viz., $\mathbf{q}=(-1/4, 1/2, 1/2)$, and use a supercell which is $(4\times2\times2)$ times the original crystallographic unit cell with 192 atoms. We use a plane-wave energy cutoff of 500 eV and k-space sampling on a $1\times2\times2$ Monkhorst-Pack grid. We have checked our calculations on a finer k mesh $1\times4\times4$ and the results hardly changed indicating the chosen k mesh to be adequate. All structural relaxations are carried out till Hellman-Feynman forces became less than 0.01 eV/Å. For x-ray absorption spectroscopy (XAS), polycrystalline $MnWO_4$ is synthesized by a solid-state synthesis route.[24] Powder x-ray diffraction established that the sample formed in the pure monoclinic space group $P2/c$ as reported earlier without any secondary phase. Room-temperature x-ray absorption measurements at the Mn $L_{2,3}$ of $MnWO_4$ were performed using linearly polarized synchrotron light at the circular polarization beamline, Elettra, Italy with a resolution of 0.2 eV at the Mn L_3(635 eV) edge. The XA spectrum was recorded using the total electron yield method by recording the sample drain current as a function of the photon energy. The base pressure of the chamber was about 3×10^{-10} mbar; clean sample surfaces were exposed for experiments by scraping the sample surface *in situ* with a diamond file.

Total energy calculations are carried out for the ferromagnetic, $\mathbf{q}=(0,0,0)$, antiferromagnetic, $\mathbf{q}=(\frac{1}{2},0,0)$, AF1 and AF2 with $\mathbf{q}=(\frac{1}{4},\frac{1}{2},\frac{1}{2})$ states of $MnWO_4$. Our calculated results both within LDA and LDA+U reveal that the antiferromagnetic state AF1 has the lowest energy in agreement with experiment. The energy difference ΔE between AF1 and the FM, AFM, and AF2 is calculated to be 0.17, 0.16, 0.01 eV/f.u., respectively, with $U=4$ eV. In the AF2 phase, the computed magnetic moment is 4.57μB with same U and rotate in a plane as described earlier. Calculations with different U parameters gave average Mn magnetic moments of $4.30\mu_B(U=0$ eV) and $4.67\mu_B(U=6$ eV), suggesting a rather weak dependence of magnetic moment on U. All magnetic states are found to be insulating both in the LDA and LDA+U method. The band gap in the AF1 state is calculated to be 1.19 eV with LDA and 2.16 eV with LDA+U which is comparable to the experimentally reported band gap of 3 eV from photoelectron measurements.[25]

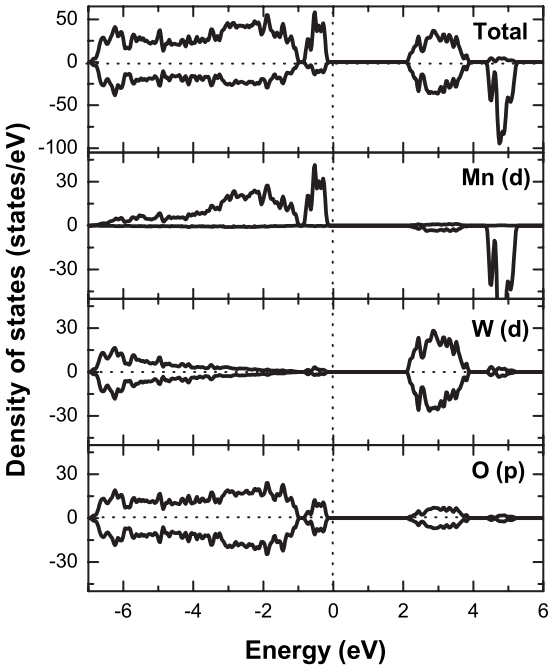

FIG. 2. Calculated total and partial density of states within LDA+U for $MnWO_4$ in the AF1 phase. All energies are measured with respect to the Fermi level. Majority and minority states are plotted on the positive and negative axes, respectively

To gain insights into the electronic structure of $MnWO_4$, the total and site projected density of states (DOS) for $MnWO_4$ in the AF1 phase calculated within LDA+U for a particular sublattice are displayed in Fig. 2. From the figure we gather that, the majority Mn d states are completely occupied while the minority states are completely empty, consistent with the Mn^{2+} valence of Mn with a nominal $3d^5$ configuration. O p states are completely occupied while the W states are completely empty, indicating the valence of W to be W^{6+}, consistent with experimental results. The Mn d states are split by the crystal field, however, the distortion of the octahedra may allow for the mixing among the states. The exchange splitting dominates the crystal-field splitting favoring the high spin configuration of Mn. The d^5 electronic configuration of Mn favors the antiferromagnetic configuration in the AF1 phase as found in our total energy calculations.

Next we calculated the polarization using the Berry phase method[26] as implemented in VASP.[22] Electric polarization in the AF2 phase with centrosymmetric crystal (wolframite) structure in the absence of SOI is found to be zero, as should be expected. This provides a clear evidence that symmetric exchange striction effects do not offer an explanation for the origin of ferroelectric polarization in $MnWO_4$. When SOI is turned on, one expects the broken inversion symmetry in the spin sector to be communicated to the spatial (charge) degrees of freedom, and indeed our calculations confirm this. In the experimental structure with SOI the computed electric polarization is $P=42.02$ $\mu C/m^2$ along the b direction. Both the magnitude and the direction of the polarization is in excellent agreement with the experimental value of $50-60$ $\mu C/m^2$.[9,16] The importance of SOI for ferroelectric

polarization in this material is also found in a recent *ab initio* calculation.[27] We found zero polarization in the collinear AF1 phase even in the presence of SOI suggesting that the spiral magnetic order is crucial for the realization of this finite (and large) electric polarization. Earlier studies[13] have shown that the relaxation of the ionic coordinates improves calculated polarization. Upon relaxation without imposing any symmetry constraints in the AF2 phase, we find the polarization in the resulting structure in absence of SOI to be $(-5.78, 4.99, 18.22)$ $\mu C/m^2$ with a magnitude of 19.75 $\mu C/m^2$. This is much smaller than the experimental value and it is also inconsistent in direction (not along b axis). However, when SOI was included in the Berry phase calculations, an additional polarization of 123.8 $\mu C/m^2$ developed along b direction. In the relaxed structure, the average deviation from the centrosymmetric position is found to be $\sim 2.7 \times 10^{-6}$ Å for Mn, while for W and O they are $\sim 2.5 \times 10^{-6}$ Å and $\sim 3.7 \times 10^{-7}$ Å, respectively. We also carried out constrained ionic relaxation calculations in which Mn and W special positions (x and z coordinates) were kept fixed. In this case, polarization without SOI remains zero while it is $(0, 121.9, 0)$ $\mu C/m^2$ in presence of SOI. The largest deviation from centrosymmetric positions is now less than $\sim 2 \times 10^{-6}$ Å. Such tiny displacements in both the cases (unconstrained and constrained ionic relaxations) are hardly detectable in any experiment and possibly their effects are swamped by zero-point vibrational effects.[13]

From the above discussion we conclude that our *ab initio* calculation offers clear evidence that spin-orbit interaction alone can account for the origin of polarization in $MnWO_4$ without involving any structural effects, establishing an electronic mechanism as the origin of ferroelectricity in this compound. Since Mn^{2+} in the high spin state ($d^5, S=5/2$) has $L=0$ in the free ion state, where the orbital moment is expected to be quenched, an induced mechanism either due to mixing of the ligand p orbitals or t_{2g}-e_g orbitals is possibly operative on this system. Indeed, band-structure results provide evidence for substantial oxygen p-Mn d mixing (Fig. 2) as well as finite t_{2g}-e_g mixing (not shown here) in partial densities of states. The orbital moment is found to be tiny $(0.001\mu_B)$ but in the same direction as the spin moment indicating Mn $3d$ states are more than half-filled.[28] However it is difficult to estimate quantitatively the extent of Mn $3d$ occupancy or its deviation from the ionic d^5 state in terms of such *ab initio* band-structure calculations since the association of the electronic charge with an atomic center within this approach is dependent on the somewhat arbitrary space partitioning and thus, leading to nonuniqueness. Within this approach, it is also not possible to estimate the expectation value of the angular momentum associated with the deviation of the Mn $3d$ occupancy from the half-filling. High-energy electron spectroscopies such as x-ray absorption spectroscopy, on the other hand, are particularly suited to provide a well-defined estimate of the $3d$ occupancy and also the expectation value of angular momentum when analyzed in conjunction with many-electron configuration interaction model.[29,30]

The XA spectrum is shown in Fig. 3. In view of the limitation in the *ab initio* simulation of XA spectrum for complex oxides,[31] we have carried out configuration interaction

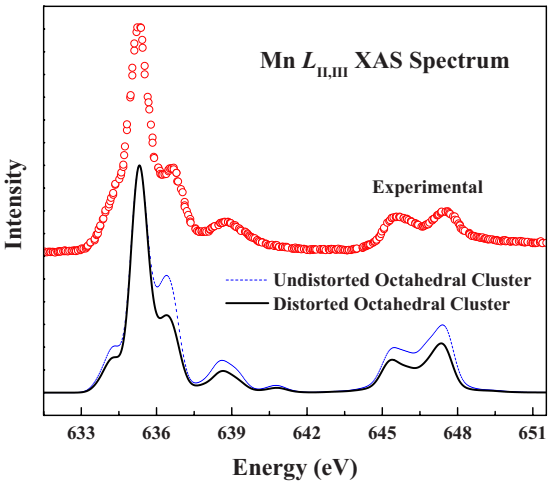

FIG. 3. (Color online) Experimental and calculated XAS spectra for $MnWO_4$.

(CI) calculations using Lanczos iterative algorithm for the distorted octahedral $(MnO_6)^{10-}$ cluster found in the real crystal for the analysis of the Mn $L_{2,3}$ XA spectrum. Since a proper consideration of the orbital-dependent Coulomb interaction between the core hole and the d electrons ($U^{dc}_{\alpha\beta\gamma\delta}$) as well as those within the $3d$ levels ($U^{dd}_{\alpha\beta\gamma\delta}$) is crucial for the description of the XA spectrum, CI calculations with full multiplet Coulomb interactions are ideally suited for the simulation of XA spectrum. The distorted cluster is characterized by pairs of three different Mn-O bond lengths, namely, 2.285 Å, 2.160 Å, and 2.104 Å, respectively. Triply degenerate $2p$ valence orbitals are considered on the oxygen atoms as well as $2p$ core and $3d$ valence orbitals on the Mn atom to calculate the $2p \rightarrow 3d$ XA process. The calculation details can be found in Ref. 29. The Hamiltonian used for the calculation includes the on-site Mn $3d$-$3d$ and $2p$-$3d$ Coulomb multiplet interactions, characterized by average values U_{dd} and U_{pd}, respectively, spin-orbit interactions on Mn $2p$ and $3d$ levels, a bare ionic octahedral crystal field $(10Dq)$ on the Mn atom, hopping interaction energies between Mn $3d$ and O $2p$ levels, parametrized in terms of Slater Koster parameters, $pd\sigma$ and $pd\pi$ ($|pd\pi| = 1/2|pd\sigma|$ as the usual convention) to account for the covalency effects and also scaled with asymmetric Mn-O bond distances $R_{\text{Mn-O}}$ as $(R_{\text{Mn-O}})^{-4}$. Charge-transfer energy Δ between O $2p$ and Mn $3d$ orbitals is defined as $E(d^{n+1}\underline{L}^1) - E(d^n)$, where $E(d^n)$ is the multiplet averaged energy of n-electron occupancy at Mn $3d$ levels and $E(d^{n+1}\underline{L}^1)$ denotes the same for a configuration obtained by transferring one electron from one of the O $2p$ levels to Mn $3d$ level having $n=5$ electrons, corresponding to the formal Mn^{2+} ion in this compound. The basis size was confined to allow a maximum of two-electron excitations on the Mn $3d$ level; in spite of this restriction, the dimensions of the Hamiltonian matrices involved are as large as 197 280. According to the usual convention, the value of U_{pd} is taken to be $1.1 \times U_{dd}$.[32]

The two regions of the experimental Mn $L_{2,3}$ XA spectrum of $MnWO_4$ around 635 and 646 eV in Fig. 3, correspond to Mn $2p_{3/2}$ and $2p_{1/2}$ spin-orbit split components, respectively. The line shape of the experimental Mn $L_{2,3}$ XA

spectrum is reproduced very well by the calculated spectrum (solid line in Fig. 3) with U_{dd}=4.0 eV, Δ=7.0 eV, $10D_q$ =0.5 eV, and $pd\sigma$=−1.29 eV. In Fig. 3, we have also shown (dotted line) the calculated XAS spectrum with same parameters, but for an undistorted $(MnO_6)^{10-}$ cluster, to illustrate the sensitivity of XAS lineshape even to such small distortions that play an important role in giving rise to the unusual magnetic and electric polarization in this material. The ground-state wave function for the true distorted structure with this set of optimal parameters is found to have an average $3d$ occupancy, n_{3d}, of 5.14, with 86.48% d^5 character, 12.99% $d^6\underline{L}^1$ character, and only 0.52% $d^7\underline{L}^2$ character, justifying the choice of the basis to be upto two electron excitations over the basic ionic configuration. Similarly the expectation value of the orbital angular momentum for the ground state is calculated to be 0.51. Thus, our x-ray absorption experiment conclusively establish a significant population of Mn $3d$ level and a consequent finite expectation value of L, beyond the half-filling in $MnWO_4$, providing a way to understand the critical presence of SOI and consequent finite polarization in this compound.

In conclusion, our first-principles electronic-structure calculations not only correctly reproduce the electronic and magnetic ground state of $MnWO_4$ but also provide an accurate estimate of the value of the ferroelectric polarization. In addition, we find that the polarization develops only in the spin spiral AF2 state driven by the spin-orbit interaction. XA spectroscopy establishes quantitatively a significant population of Mn $3d$ states beyond the half-filling and a nonzero expectation value of the orbital angular momentum due to the presence of sizable hopping interactions providing an insight into the significant presence of spin-orbit coupling in this system.

I.D, and D.D.S. thanks DST, India for financial support.

[1] T. Kimura *et al.*, Nature (London) **426**, 55 (2003).
[2] N. A. Spaldin and M. Fiebig, Science **309**, 391 (2005).
[3] S.-W. Cheong and M. Mostovoy, Nature Mater. **6**, 13 (2007).
[4] L. C. Chapon, P. G. Radaelli, G. R. Blake, S. Park, and S.-W. Cheong, Phys. Rev. Lett. **96**, 097601 (2006).
[5] Y. J. Choi, H. T. Yi, S. Lee, Q. Huang, V. Kiryukhin, and S. W. Cheong, Phys. Rev. Lett. **100**, 047601 (2008).
[6] H. Katsura, N. Nagaosa, and A. V. Balatsky, Phys. Rev. Lett. **95**, 057205 (2005).
[7] G. Lawes *et al.*, Phys. Rev. Lett. **95**, 087205 (2005).
[8] Y. Yamasaki, S. Miyasaka, Y. Kaneko, J. P. He, T. Arima, and Y. Tokura, Phys. Rev. Lett. **96**, 207204 (2006).
[9] K. Taniguchi, N. Abe, T. Takenobu, Y. Iwasa, and T. Arima, Phys. Rev. Lett. **97**, 097203 (2006).
[10] M. Mostovoy, Phys. Rev. Lett. **96**, 067601 (2006).
[11] C. Jia, S. Onoda, N. Nagaosa, and J. H. Han, Phys. Rev. B **76**, 144424 (2007).
[12] I. A. Sergienko and E. Dagotto, Phys. Rev. B **73**, 094434 (2006).
[13] H. J. Xiang and M.-H. Whangbo, Phys. Rev. Lett. **99**, 257203 (2007).
[14] A. Malashevich and D. Vanderbilt, Phys. Rev. Lett. **101**, 037210 (2008).
[15] H. J. Xiang, S.-H. Wei, M.-H. Whangbo, and J. L. F. Da Silva, Phys. Rev. Lett. **101**, 037209 (2008).
[16] A. H. Arkenbout, T. T. M. Palstra, T. Siegrist, and T. Kimura, Phys. Rev. B **74**, 184431 (2006).
[17] O. Heyer *et al.*, J. Phys.: Condens. Matter **18**, L471 (2006).
[18] B. Kundys, C. Simon, and C. Martin, Phys. Rev. B **77**, 172402 (2008).
[19] A. Daoud-Aladine, B. Kundys, C. Martin, P. G. Radaelli, P. J. Brown, C. Simon, and L. C. Chapon, Phys. Rev. B **80**, 220402(R) (2009).
[20] G. Lautenschläger, H. Weitzel, T. Vogt, R. Hock, A. Bohm, M. Bonnet, and H. Fuess, Phys. Rev. B **48**, 6087 (1993).
[21] H. Ehrenberg, H. Weitzel, H. Fuess, and B. Hennion, J. Phys.: Condens. Matter **11**, 2649 (1999).
[22] G. Kresse and J. Hafner, Phys. Rev. B **47**, 558 (1993).
[23] S. L. Dudarev, G. A. Botton, S. Y. Savrasov, C. J. Humphreys, and A. P. Sutton, Phys. Rev. B **57**, 1505 (1998).
[24] D. H. Choi and C. S. Kim, J. Appl. Phys. **103**, 07E316 (2008).
[25] T. Ejima *et al.*, J. Lumin. **119-120**, 59 (2006).
[26] R. D. King-Smith and D. Vanderbilt, Phys. Rev. B **47**, 1651 (1993).
[27] C. Tian, C. Lee, H. Xiang, Y. Zhang, C. Payen, S. Jobic, and M. H. Whangbo, Phys. Rev. B **80**, 104426 (2009).
[28] O. Eriksson, A. M. Boring, R. C. Albers, G. W. Fernando, and B. R. Cooper, Phys. Rev. B **45**, 2868 (1992).
[29] P. Mahadevan and D. D. Sarma, Phys. Rev. B **61**, 7402 (2000).
[30] D. D. Sarma, J. Phys. Soc. Jpn. **65**, 1325 (1996).
[31] O. Wessely *et al.*, Phys. Rev. B **68**, 235109 (2003).
[32] S. R. Barman and D. D. Sarma, Phys. Rev. B **49**, 13979 (1994).